Site-testing results by means of an aerosol, backscatter lidar at the Roque de los Muchachos Observatory

Michaël Sicard

Universitat Politècnica de Catalunya / Institut d'Estudis Espacials de Catalunya, Dept. of Signal Theory and Comunications, Remote Sensing Lab., c/ Jordi Girona, 1-3, E-08034, Barcelona, Spain
msicard@tsc.upc.edu

M. Nadzri Md Reba

Universitat Politècnica de Catalunya / Institut d'Estudis Espacials de Catalunya, Dept. of Signal Theory and Comunications, Remote Sensing Lab., c/ Jordi Girona, 1-3, E-08034, Barcelona, Spain
nadzri@tsc.upc.edu

Sergio Tomás

Universitat Politècnica de Catalunya / Institut d'Estudis Espacials de Catalunya, Dept. of Signal Theory and Comunications, Remote Sensing Lab., c/ Jordi Girona, 1-3, E-08034, Barcelona, Spain
tomas.martinez@tsc.upc.edu

Adolfo Comerón

Universitat Politècnica de Catalunya, Dept. of Signal Theory and Comunications, Remote Sensing Lab., c/ Jordi Girona, 1-3, E-08034, Barcelona, Spain
comeron@tsc.upc.edu

Oscar Batet

Universitat Politècnica de Catalunya, Dept. of Signal Theory and Comunications, Remote Sensing Lab., c/ Jordi Girona, 1-3, E-08034, Barcelona, Spain
oscar.batet@tsc.upc.edu

Constantino Muñoz-Porcar

Universitat Politècnica de Catalunya, Dept. of Signal Theory and Comunications, Remote Sensing Lab., c/ Jordi Girona, 1-3, E-08034, Barcelona, Spain
constan@tsc.upc.edu

Alejandro Rodríguez

Universitat Politècnica de Catalunya, Dept. of Signal Theory and Comunications, Remote Sensing Lab., c/ Jordi Girona, 1-3, E-08034, Barcelona, Spain
alejandro@tsc.upc.edu

Francisco Rocadenbosch

Universitat Politècnica de Catalunya / Institut d'Estudis Espacials de Catalunya, Dept. of Signal Theory and Comunications, Remote Sensing Lab., c/ Jordi Girona, 1-3, E-08034, Barcelona, Spain
roca@tsc.upc.edu

Casiana Muñoz-Tuñón

Instituto de Astrofísica de Canarias, c/ Vía Láctea s/n, E-38205, La Laguna, Tenerife, Spain
casiana@iac.es

Jesús J. Fuensalida

Instituto de Astrofísica de Canarias, c/ Vía Láctea s/n, E-38205, La Laguna, Tenerife, Spain
fuensalida@iac.es

ABSTRACT

The Roque de los Muchachos Observatory, located on the island of La Palma in the Canary Islands, is home of many astronomical facilities for its high sky quality. In the context of the Extremely Large Telescope Design Study, two intensive lidar campaigns were performed at the Roque de los Muchachos Observatory near the Jacobus Kapteyn Telescope between 9th and 11th July 2007 and between 26th May and 14th June 2008. The goal of the campaign was to characterize the atmosphere in terms of planetary boundary layer (PBL) height and aerosol stratification vs. synoptic conditions. Three typical synoptic situations were found which, respectively, privileged the intrusion of aerosols from marine/oceanic, anthropogenic and Saharan origin. All measurements revealed a multi-layer stratification with a mean PBL height of 546 ± 198 m agl and top layers as high as ~ 8400 m asl. As a by-product an estimate of the aerosol optical thickness was also obtained and compared to the total atmospheric extinction coefficient measured by the Carlsberg Meridian Telescope. Except in the presence of Saharan dust the aerosol optical thickness is very low: the average values are 0.0405 at 532 nm and 0.0055 at 1064 nm. In the presence of Saharan dust values of 0.233 and 0.157 were found at 532 and 1064 nm, respectively. The proportion of aerosol optical thickness contained in the layers above the PBL against that contained in the PBL is in all cases greater or equal to 50 % which emphasizes the importance of the upper layers in the scattering and absorption of astronomical signals. Additionally, for the first time spaceborne lidar measurements were also compared to a ground lidar for evaluating the use of a spaceborne active instrument for aerosol content monitoring in an astronomical site.

Keywords: site testing; atmospheric effects; scattering; instrumentation: miscellaneous; methods: data analysis

1. INTRODUCTION

The Roque de los Muchachos Observatory (ORM), located in the municipality of Garafía on the northern part of the island of La Palma in the Canary Islands, is home of many astronomical facilities belonging to the European Northern Observatory. Most aerosols reaching the island of La Palma can be classified into three types: marine/oceanic, anthropogenic (from Europe or North America mixed with marine/oceanic aerosols) or African (Sahara and Sahel) aerosols (Varela et al. 2008). The atmospheric aerosols have two great impacts on the quality of astronomical observations: the extinction and the astronomical *seeing* .

The extinction due to atmospheric aerosols quantifies the absorption and the scattering of incoming radiation. Generally it depends on the wavelength of the incoming radiation and the aerosol size, shape, composition and refractive index. At ORM, the Carlsberg Meridian Telescope (CMT), described later in this paper, provides a daily measurement of the atmospheric extinction since 1984. The analysis of this public database provides very important statistical results, among them the percentage of nights affected by Saharan dust (Guerrero et al. 1998; García-Gil et al. 2009). It is well known that Saharan dust can reduce significantly the visibility (and therefore the quality of astronomical observations) because of their strong extinction properties. After the analysis of more than 20 years of the database García-Gil et al. (2009) concludes that about 30 % of the nights in summer are affected by African dust – 20 % during the rest of the year. For the remaining nights (which represent at least 70 % of them) only marine/oceanic and anthropogenic (mixed with marine/oceanic aerosols) aerosols are present. The effect of those two aerosol types is not so well characterized and especially their vertical distribution and their effect on the quality of the observations are not known. The latter statement is also true for Saharan dust.

The astronomical *seeing* , not estimated in this work, gives the size of a point source at the telescope focus. It is directly related to the measurement of the refractive index structure constant, usually noted C_n^2, which gives a quantitative information on the stability of the atmospheric layers. The latter parameter is a measurement of the optical turbulence.

Active remote sensing instruments such as lidars (Light Detection and Ranging), which are sensitive to scattering by micrometer and submicrometer particles, are the ideal system to measure the aerosol extinction and vertical distribution. In the context of the Extremely Large Telescope (ELT) Design Study two lidar intensive field campaigns (IFC) were performed in the ORM near the Jacobus Kapteyn Telescope (17°52'41.2" W, 28°45'40.1"N, 2395 m asl) between 9th and 11th July 2007 and between 26th May and 14th June 2008 (hereinafter noted as 09JUL07 – 11JUL07 and 26MAY08 – 14JUN08, respectively). The goal of the IFCs was 1) to characterize the atmosphere in terms of planetary boundary layer (PBL) height and aerosol stratification vs. synoptic conditions, and 2) to correlate the atmospheric structure with astronomical parameters tracers of the visibility. As a by-product an estimate of the aerosol optical thickness (*AOT*) was also obtained and compared to the total atmospheric extinction coefficient measured by the CMT. As an attempt to evaluate the use of a spaceborne active instrument for aerosol content monitoring in an astronomical site the ground lidar profiles were also compared to those of a spaceborne lidar.

The paper is organized as follows: Section 2 describes the instrumentation and the method used in the study; Section 3 describes the synoptic conditions found during both IFCs and the air mass origins resulting from them; Section 4 gives the results of the aerosol stratification in ORM; and finally Section 5 presents a discussion of the aerosol loading and its relation with the stratification, and the comparison of the ground lidar with both the CMT instrument and a spaceborne lidar.

2. INSTRUMENTATION

In 2007 two full nights and an afternoon of measurements are available. In 2008, the measurements effectively started after set-up and setting on the night of 27MAY08 and ended on the morning of 14JUN08, i.e. over a period of 16 nights (during 2 nights, 30MAY08 and 31MAY08, the measurements had to be aborted because of low clouds at ground level). The method employed to retrieve the aerosol stratification as well as the *AOT* by-product is based on nocturnal cycle measurements by means of the aerosol, backscatter liar from the Universitat Politècnica de Catalunya (UPC). Measurements from collaborative close-by instruments, as well as model and satellite tools are also used.

2.1 Lidar

The UPC lidar is based on a frequency-doubled Nd:YAG laser delivering simultaneously pulses of approximately 160 mJ and 7-ns duration at 1064 and 532 nm (Rocadenbosch et al. 2002). The backscattered light is collected by an 8-inch diameter Schmidt-Cassegrain telescope and focused on one end of an optical-fiber bundle. At the other end of the bundle dichroic beamsplitters deflect the collected light towards one of three photodetectors according to the wavelength. An avalanche photodiode-based receiver is used for the 1064-nm channel. Photomultiplier tube-based receivers are used for both the 532- and the 607.4 nm channels, the latter corresponding to the Raman shift of the incident radiation at 532 nm produced by the atmospheric nitrogen. The system full overlap factor is reached at approximately 300 – 400 m.

The lidar was shipped from Barcelona to the Canary Islands by boat and installed in ORM near the Jacobus Kapteyn Telescope (17°52'41.2" W, 28°45'40.1"N, 2395 m asl). The nocturnal cycle measurements consist of static measurements of usually 60-min. duration in a zenith line of sight (LOS) with a 1-min. resolution. The retrieved

parameters are: vertical aerosol distribution, PBL height, AOT and extinction and backscatter coefficient profiles. Some information on the lidar ratio (LR), defined as the extinction-to-backscatter ratio, and also on the Ångström exponent (AE), which describes the spectral dependency of the AOT , can also be deduced. Between two wavelengths λ_1 and λ_2 AE is defined as follows:

$$AE = -\frac{\ln\left[\frac{AOT(\lambda_1)}{AOT(\lambda_2)}\right]}{\ln\left[\frac{\lambda_1}{\lambda_2}\right]}. \quad (1)$$

In the context of aerosols the PBL is defined as the part of the troposphere that is directly influenced by the presence of the earth's surface, and responds to surface forcings with a timescale of about an hour or less (Stull 1988). Because the aerosols formed at the ground level are confined in the PBL it exists a marked transition in terms of concentration between the PBL and the troposphere above. As the optical power measured by a lidar is proportional to the aerosol concentration the lidar signal reflects that marked transition in form of a strong negative gradient. Here the retrieval of the PBL was made using the gradient method (Sicard et al. 2006) which looks for the absolute negative minimum of the first derivative which corresponds to the strongest negative gradient of the lidar signal. The mean PBL height was calculated with a time resolution of 30 min. and its error bar was computed as the standard deviation of the 30 profiles used to calculate the mean PBL height. All profiles were visually inspected and the resulting PBL height was cross-compared to the previous and the following value in order to guarantee temporal coherency of its evolution. The retrieval of the height of the highest aerosol layer, called hereinafter top layer (TL), was performed with an adaptation of the gradient method applied to the region of weak but non-zero signal just below the free troposphere.

The profiles of the aerosol optical coefficient (backscatter and extinction) were retrieved by means of the Klett-Fernald-Sasano (KFS) method (Klett 1981; Fernald 1984; Sasano & Nakane 1984) using a constant lidar ratio. Unfortunately, the Raman inversion method (Ansmann et al. 1992) could not be applied because of too low signal-to-noise ratios in the Raman channel in both IFCs.

The AOT was measured by integrating the aerosol extinction coefficient profile from the minimum height of confidence, usually between 300 and 400 m agl, and up to the free troposphere, more concretely up to a height which is above the highest layer detected. The extinction coefficient profile not "seen" by the lidar because of its overlap factor (below 300 – 400 m agl) was taken as the extrapolation of the extinction profile at the minimum height of confidence.

Table 1 shows the schedule of the static measurements performed by the lidar. A total of 37 usable measurements of usually 30-min. and 60-min. duration in 2007 and 2008, respectively, were performed. In some cases coinciding with the overpass of the CALIOP (Cloud-Aerosol Lidar with Orthogonal Polarization) lidar on board of CALIPSO (Cloud-Aerosol Lidar and Infrared Pathfinder Satellite Observation) (Winker, Pelon & McCormick 2006), the measurements were extended to 150 min. Two and seven CALIPSO overpasses coincided in 2007 and 2008, respectively, within a time frame of ± 2 hours. In Section 5.3 a comparison between both ground and spaceborne lidars is presented. To our knowledge it is the first time that the contribution of a spaceborne active instrument is studied to characterize an astronomical site.

2.2 Ground and spaceborne collaborative instruments

The Carlsberg Meridian Telescope, situated a few hundreds meters away from the UPC lidar, provides nightly values of the total extinction coefficient (TEC) in the Sloan Digital Sky Survey (SDSS) r' band at $\lambda_{r'} = 625\ nm$ derived from CCD frames obtained through the observations of an average of 30 to 40 photometric standard stars per night. Since the type of aerosol observed above ORM is supposedly not known, the conversion of TEC at $\lambda_{r'}$ into AOT at λ_{lidar} is not straightforward. For that reason the comparison between both the lidar and the CMT measurements is made in terms of total optical thickness, TOT. The calculation of TEC at $\lambda_{lidar} = 532\ nm$ is made as follows. First the aerosol extinction coefficient (AEC) is calculated using the formula (King 1985):

$$AEC = TEC(\lambda_{r'}) - MEC(\lambda_{r'}), \tag{2}$$

where $MEC(\lambda_{r'}) = 0.0734\ mag{\cdot}airmass^{-1}$ represents the molecular extinction coefficient at $\lambda_{r'}$. $MEC(\lambda_{r'})$ can be extracted from a look-up table also given in King (1985). According to Jones (1984) in the range [300; 1100 nm] AEC in ORM can be considered, to a first approximation, independent of the wavelength and therefore TEC can be expressed at any wavelength as:

$$TEC(\lambda) = AEC + MEC(\lambda) = TEC(\lambda_{r'}) - MEC(\lambda_{r'}) + MEC(\lambda). \tag{3}$$

At $\lambda_{lidar} = 532\ nm$, $MEC(\lambda_{lidar}) = MEC(530\ nm) = 0.1087\ mag{\cdot}aimass^{-1}$. Finally $TOT(\lambda_{lidar})$ is obtained by simply changing the units of $TEC(\lambda_{lidar})$ **from [mag·aimass^{-1}] to no unit by dividing by** 1.086 mag·aimass^{-1}.

In situ meteorological information of ground pressure, temperature, and humidity, as well as wind speed and direction were provided by the weather station of the Isaac Newton Group of Telescopes (ISGT) situated a few hundreds meters away from the UPC lidar.

As mentioned previously CALIOP data were also considered to evaluate the use of a spaceborne active instrument for aerosol content monitoring in an astronomical site. CALIOP Level 1 data products were compared to the UPC lidar profiles in terms of attenuated backscatter profiles. Out of the overpass track of the CALIPSO satellite the 120 nearest points (pulses) to the ground lidar were integrated. At the pulse repetition frequency of CALIOP (20 Hz) and at the speed of the satellite, this is equivalent to an integration time of 6 s and a ground track of 40 km. Being aware that the aerosol products reported in the Level 2, version 2.01, release of the CALIOP profile products are beta-quality data products and not appropriate for scientific publication, no comparison of aerosol products was attempted.

Images of MODIS (Moderate Resolution Imaging Spectroradiometer) aboard AQUA satellite were also used to confirm or discard the presence of Saharan dust during the two campaigns.

2.3 Modeling

Mean synoptic maps of sea level pressure were generated from the NCEP-NCAR (National Centers for Environmental Prediction–National Center for Atmospheric Research) reanalysis project (Kalnay et al. 1996).

Backtrajectories from HYSPLIT (the Hybrid Single Particle Lagrangian Integrated Trajectory Model) (Draxler & Rolph 2003; Rolph 2003) were provided by NOAA – ARL (National Oceanic and Atmospheric Administration – Air Resources Laboratory) and used to check the air masses origin.

The DREAM (Dust Regional Atmospheric Model) (Nickovic et al. 2001) model was used in the same goal as MODIS to confirm or discard the presence of Saharan dust during the two campaigns, but also as a forecast of the vertical distribution of Saharan dust by means of height-resolved vertical cross sections of dust concentration.

3. METEOROLOGICAL SCENARIOS

According to a thorough study of the day-after-day evolution of synoptic maps of the sea level pressure provided by the NCEP–NCAR reanalysis project (Kalnay et al. 1996), it is possible to distinguish three main synoptic patterns during the two IFCs: 9JUL07 – 11Jul07 (IOP1, Intensive Observation Period 1), 27MAY08 – 02JUN08 (IOP2) and 03JUN08 – 14JUN08 (IOP3). Fig. 1 shows the average map at 0000 UTC for the three periods. During IOP1 (Fig. 1a) a strong anticyclone (up to 1032 mb) is situated west of the Iberian Peninsula while a large but moderate low pressure system is installed over North Africa. This situation supports the intrusion of Saharan dust that was indeed observed by the lidar. The image of MODIS aboard AQUA satellite on 11JUL07 at 1415UTC, i.e. at the end of the first IFC, shown in Fig. 2 demonstrate the presence of Saharan dust over ORM. DREAM forecasts of the *AOT* at 550 nm (presented later in the paper) also clearly confirm the presence of Saharan dust above ORM during IOP1. The first half of the second IFC, IOP2, (Fig. 1b) was dominated by a stable anticyclone situation centred on the Azores islands or slightly southwest of them, a situation that can possibly be considered typical. In the second half of the campaign, IOP3, (Fig. 1c) a new high pressure system coming from the Caribbean pushed the Azores anticyclone northeast towards Western Europe.

These three situations bring air masses from different origin and identified according to (Varela et al. 2008) as African (dust and mineral aerosols) during 09JUL07 – 11JUL07, Atlantic (marine and oceanic aerosols) during 27MAY08 – 02JUN08 and European (anthropogenic emissions from sulfates and carbon) during 03JUN08 – 14JUN08. **Following that classification, the assumption is made that the *LR* (necessary for the lidar inversion by the KFS method) during IOP1 is ~ 60 sr corresponding to mineral dust (Mona et al. 2006; Papayannis et al. 2008), and that it is ~ 30 sr for the other two IOPs corresponding to marine aerosols (Ansmann & Müller 2005; Doherty et al. 1999; Sicard 2000) which is the dominant aerosol type during IOP2 and IOP3 when the synoptic conditions do not favour long-range transport from North Africa.** This is indeed the only assumption made on the type of aerosol in this paper.

4. AEROSOL STRATIFICATION IN ORM

The temporal evolution of the range-square corrected signal (RSCS) at 1064 nm during the 16 nights of IOP2 and IOP3 has been shown in detail in Sicard et al. (2009). Here only one representative nocturnal cycle is represented for each of the three situations identified: on 09JUL07 (Fig. 3a), on 02JUN08 (Fig. 3b) and on 11JUN08 (Fig. 3c). The choice for representing the 1064-nm channel profiles comes from the higher contrast between aerosols and molecules that offers that wavelength compared to 532 nm. Another issue to take into account for interpreting correctly those three figures is that the colour bar scale is adjusted for every night in order to emphasize the signal variations in the PBL. Consequently according to the state of the PBL the molecular region (aerosol-free) appears or blue or yellow-green. The 30-min. mean PBL height and its error bar is indicated by '+' signs. The main feature is that all nights show a multi-layer stratification and Fig. 3 is representative of that feature: during IOP1 (Fig. 3a) several layers of Saharan dust were observed above the PBL up to almost 5 km agl, during IOP2 (Fig. 3b) a single layer is detected above the PBL while during IOP3 (Fig. 3c) several thin layers are observed up to 4.5 km agl. During IOP1 the Saharan dust layer on top of the PBL at ~ 1 km is sometimes misleading the algorithm in retrieving the correct PBL height, hence the large error bars seen in Fig. 3a.

Fig. 4 shows the temporal evolution of the PBL and the TL heights for all 37 measurements performed during both IFCs. One sees clearly that during both IFCs the nocturnal cycles show in general a low nocturnal PBL sometimes as low as 250 m agl but which in any case never exceeds 1000 m agl. **Even though the full overlap of the UPC lidar is not reached until 300 – 400 m agl, the PBL height can still be retrieved at lower altitudes if the gradient is strong and predominates compared to the overlap increase. The bottom limit is fixed by the blind zone of both the reception and emission fields of view (less than 200 m).** The mean values of the PBL and the TL heights and their associated standard deviations are given in Table 2 in the column labelled "Layer height" for the three IOPs. For the PBL an overall mean height of 546 ± 198 m agl is calculated. If compared to other coastal regions with much more anthropogenic activities and consequently more contamination such as Barcelona where the diurnal PBL varies between 300 and 1450 m in summer (Sicard et al. 2006), this height is not especially low. During IOP1, IOP2 and IOP3 the mean PBL height is around 581 ± 186, 487 ± 192 and 571 ± 204 m agl, respectively. The relatively high standard deviations found indicate a strong spatial variability of the PBL. During IOP2 the stable synoptic situation supports a shallower development of the PBL compared to the other two IOPs. This is also supported by the temperature and wind speed measurements at ground level performed at the INGT meteorological station. During IOP2 and IOP3 the temperature oscillated between 5 and 12 ºC, and between 10 and 17 ºC, respectively, and the wind speed between 10 and 50, and 0 and 30 $km \cdot h^{-1}$. Low temperatures usually create a negative buoyancy effect and relatively strong winds prevent or at least reduce the vertical development of air masses. The PBL heights found in ORM are slightly higher than measurements made a few days before IOP1 by Sicard et al. (2008) in the Teide Observatory on the neighbouring island of Tenerife at 2400 m asl where the PBL heights fluctuated between 375 and 810 m agl. **The small dimension of La Palma compared to Tenerife and the exceptionally steep orography of the island (ORM is at 2395 m asl and at less than 9 km from the coast) can partially explain this difference: if the distances are short and the steepness is strong then the wind near the surface will not be horizontal but either upslope or downslope. Since the prevailing winds at ORM are from the northeast (Varela, Muñoz-Tuñon & Mahoney 1999) the wind on the ridge is generally upslope and will draw upward the air masses resulting in a higher PBL. However it is known that the height of the PBL also varies according to the atmospheric conditions. The difference observed between both campaigns at ORM and in the Teide Observatory can be due to either explanations.**

For IOP1, IOP2 and IOP3 the mean TL height is around 3268 ± 480, 1983 ± 490 and 4008 ± 970 m agl. In terms of aerosol distribution those heights are remarkably high since they correspond to 5663, 4378 and 6403 m asl, respectively. During IOP1 Fig. 4 shows a fast sedimentation of the Saharan dust layer from a TL height of ~ 5 km down to less than 2 km. During IOP2 the same feature as for the PBL is observed: a shallower development of the air masses above the PBL. During IOP3 a strong spatial variability is observed as well as heights extremely high up to ~ 8400 m asl.

In order to check the air masses origin which were claimed in Section 3 HYSPLIT backtrajectories were run coinciding with the lidar measurement starting at 2302UTC on 09JUN07 (Fig. 5a), at 0140UTC on 03JUN08 (Fig. 5b) and at 0119UTC on 12JUN08 (Fig. 5c). The arriving heights were 500, 2500 and 3500 m, except for IOP2 (500, 1000 and 1500 m) because of lower aerosol vertical extension during that period. **On the one hand, during IOP1 (Fig. 5a) North Africa is clearly identified as the origin of the air masses arriving at ORM at 2500 and 3500 m on 09JUN07, and during IOP2 (Fig. 5b) the backtrajectories clearly show that the air masses had only travelled above the Atlantic Ocean which coincides with the assumption of the Atlantic origin formulated earlier. On the other hand for IOP3 the classification of air masses according to the synoptic situation is not as clearly depicted. Fig. 5c does not show that the air masses on 12JUN08 had travelled over Europe as claimed earlier. As the accuracy of the backtrajectories simulated by HYSPLIT decreases with the steepness of the orography around the endpoint and**

with the altitude, one more HYSPLIT run was simulated (Fig. 5d). The endpoint was not chosen at ORM but at the nearest coast (17°52'41.2" W, 28°50'17.17" N, 0 m asl) which is located ~9 km North of ORM. The endpoint altitudes were chosen at 500, 1500 and 2395 m asl (the ORM altitude). This new simulation is quite different from Fig. 5c and clearly shows that the air masses are originating from Europe (Germany, France, Spain and Portugal). It is then highly probable that the air masses arriving at 2395 m asl also travelled over the ORM a little bit later.

5. AEROSOL LOADING IN ORM AND DISCUSSION

5.1 Aerosol loading in ORM

The lidar *AOT* was retrieved at both wavelengths of 1064 and 532 nm. The right hand columns of Table 2 labelled "*AOT* at 532 nm" and "*AOT* at 1064 nm" give the lidar-derived *AOT* in the PBL, above the PBL and in the whole atmospheric column which is the sum of the two previous terms. In the absence of Saharan dust, i.e. during IOP2 and IOP3, the column *AOT* is very low: 0.051 and 0.03 at 532 nm, and 0.008 and 0.003 at 1064 nm, respectively. In approximately half of the cases of IOP3 the lidar inversion at 532 nm failed. With *AOTs* as low as 0.016 (the minimum value retrieved) the lidar reaches its detection limit in the 532-nm channel: the aerosol return produces too weak signals on the order of magnitude of the error level of the inversion algorithm. During IOP1 high column *AOTs* are found due to the Saharan dust: 0.233 and 0.157 at 532 and 1064 nm, respectively.

Fig. 6 shows the temporal evolution of the column *AOT*. During IOP3 the *AOT* at 1064 nm seems to be rather constant. In spite of larger vertical distributions observed during IOP3 the *AOT* results lower than during IOP2 indicating that the highest layers do not contribute significantly to the optical thickness in the atmospheric column. Since the PBL height did not vary significantly between both periods, it also indicates that the type of aerosols contained in the PBL, or at least their optical properties, was different for both periods. Another difference observed between both periods is the behaviour of the humidity at ground level recorded by the INGT meteorological station: the average relative humidity was approximately between 50 – 75 % and below 25 % during IOP2 and IOP3, respectively. **Even though it was measured at ground level it foreshadows a similar difference in the column. The aerosol higroscopicity might explain the reason why higher** *AOTs* **were found in the first part of the campaign compared to the second period: Shettle and Fenn (1979) reported an increase of the extinction coefficient (and therefore of** *AOT* **) of marine aerosols of 20 and 40 % at 532 and 1064 nm, respectively, when the relative humidity was increased from 10 to 70 %.** A striking feature during IOP1 is that the *AOT* values are similar on 09JUL07 and 11JUL07 whereas the TL height went down from ~ 5 km to less than 2 km. **This indicates a sedimentation of the Saharan dust layers observed on 09JUL07 but without deposition. This phenomenon, rather unusual so close to the source, results in a negative effect for astronomical applications.**

A further exploration of those results is the determination of the proportion of *AOT* contained in the PBL against that contained in the other layers above the PBL. Fig. 7 shows that proportion for the three IOPs at both wavelengths. The percentage of *AOT* is very similar between both wavelengths and very different between the three IOPs. During IOP1, approximately 8 – 9 % of the column *AOT* is contained in the PBL, 50 – 54 % during IOP2 and 35 – 36 % during IOP3. **Even in the absence of Saharan dust the proportion of** *AOT* **contained in the layers above the PBL is either equal (IOP2) or larger (IOP3) than that contained in the PBL. This is a quite unusual result which indicates once again that the critical layer for good sky quality in terms of aerosol extinction is not the PBL but the aerosol layers above it.**

Representative profiles of the aerosol backscatter coefficient of each IOP are plotted in Fig. 8. As for the three HYSPLIT backtrajectory runs they correspond to the lidar measurements starting at 2302UTC on 09JUN07 (Fig. 5a), at 0140UTC on 03JUN08 (Fig. 5b) and at 0119UTC on 12JUN08 (Fig. 5c). During IOP1 and at both wavelengths the backscatter coefficient reaches high values above the PBL due to the presence of Saharan dust. In the PBL it is on the order of magnitude of the backscatter measured during IOP2 at 532 nm, and it is lower than the backscatter measured during IOP2 and IOP3 at 1064 nm. The comparison of the other two IOPs shows 1) in the PBL values lower during IOP3 than during IOP2 which is an expected result according to the above discussion and 2) above the PBL similar profiles at 1064 nm whereas at 532 nm the backscatter coefficient is lower during IOP3. This emphasizes a great variability of the aerosols' optical properties in the PBL 1) spectrally and 2) as a function of the synoptic conditions. In particular, the differences observed between IOP2 and IOP3 indicate a probable different mixing state of the aerosols especially in the PBL which results in a high spectral variability which goes against the hypothesis made in Section 2.2 that the AEC is not wavelength-dependent.

5.2 Aerosol loading compared to CMT measurements

The comparison between the lidar-derived and the CMT-derived total optical thickness at 532 nm over both IFCs is shown in Fig. 9. The minimum value of the CMT-derived *TOT* is 0.1089 and apart from this value all the others are higher than 0.1105 (equivalent to 0.12 mag·aimass^{-1}) which represents the upper limit indicating no aerosol extinction at all. Therefore the CMT confirms that the level of the extinction is very close to that of molecules and therefore that the aerosol load is very low. Additionally it also confirms the absence of Saharan dust during IOP2 and IOP3 since the *TOT* does not exceed (except in one case on 28M at 0031 UTC) the lower limit indicating the presence of Saharan dust fixed to 0.1409 (equivalent to 0.153 mag·airmass^{-1} found by Guerrero et al. (1998)). The mean value of the CMT-derived *TOT* over both IOP2 and IOP3, is 0.1172 which is a relatively large value compared to the mean value of 0.104 calculated over 15 years (1984-1998) by Guerrero et al. (1998). **Since the mean value found here was measured in summer months, this difference is consistent with the conclusion from the same authors that in summer high-extinction episodes are more frequent than the rest of the year.** The mean *TOT* over IOP2, 0.123, is slightly larger than over IOP3, 0.115 which coincides with the differences found on the lidar-derived *AOT* in Section 5.1. From Fig. 9, the lidar-derived *TOT* fluctuated between 0.123 and 0.186 while the CMT-derived *TOT* remains comparatively constant around the average value of 0.1172. No correlation is found between both quantities probably because of the mixing state of the aerosols which implies a high spectral variability which is not taken into account in the retrieval of the CMT-derived *TOT* (see Section 2.2). Varela et al. (2008) also suggested this hypothesis when comparing *TEC* with the aerosol index provided by the spaceborne OMI (Ozone Monitoring Instrument) instrument.

As far as IOP1 is concerned the correlation between lidar-derived and CMT-derived *TOT* is quite good: the correlation coefficient of the best-fit line (black straight line in Fig. 9) is 0.93. The good correlation shows that for Saharan dust the hypothesis made by the method employed by the CMT that the extinction is not wavelength-dependent is quite reasonable. However even with not so directive instruments like MODIS, the comparison between CMT-derived *TEC* and MODIS-derived *TOT* for Saharan dust aerosols also produces a reasonable agreement (Varela et al. 2008).

At this stage it is now possible to further validate the *LR* value chosen for inverting the IOP1 data. As mentioned in Section 4 the lidar inversions of the IOP1 data were realized assuming a constant *LR* of 60 sr, a typical value for mineral dust (Mona et al. 2006; Papayannis et al. 2008). This value was chosen a posteriori once the presence of Saharan dust had been checked. Now, if we consider the CMT-derived *AOT*, resulting from the subtraction of the molecular

component to the *TOT* , to be the "true" value, then it is possible to use an iterative inversion method by forcing the lidar-derived *AOT* to be equal to this "true" value (Landulfo et al. 2003). The method yields the necessary *LR* to fulfil this requirement. For IOP1 the *LR* obtained through this method is 61 ± 11 sr. It shows clearly the signature of mineral particles and, consequently, validates our initial guess. In the same way it also validates the extinction coefficient profiles at 532 and 1064 nm and therefore the resulting *AOTs* . The Ångström exponent can then be calculated between both lidar wavelengths. **Considering all points of IOP1 the mean *AE* is 0.61 ± 0.29, a value in agreement with previous studies made by Doherty et al. (1999) and Toledano et al. (2007). This relatively low value of *AE* indicates that the large *AOTs* found during IOP1 are the result of the extinction by large particles which constitute Saharan dust. In conlusion, whenever a meteorological scenario allows for the intrusion of Saharan dust, the astronomical infrared observations are affected. However, the annual percentage of nocturnal observing period affected by dust-loaded episodes is very low (Cuevas et al. 2009).**

5.3 Aerosol loading compared to CALIOP measurements

In this subsection we argue about the correlation between CALIOP profiles and the UPC ground-based lidar in order to explore the use of a spaceborne active instrument for aerosol content monitoring in an astronomical sites. Among the seven CALIPSO overpasses (selected when the overpass was within 500 km from ORM) in 2008 none of them crossed directly over the island of La Palma which is relatively narrow (28 km wide). Since no long-range transport of extraordinary aerosols (like Saharan dust) was observed during the second IFC, the seven CALIOP profiles show either a marine boundary layer below ~ 1.5 km asl or cloud already formed at that altitude (when the overpass is above the Atlantic Ocean), or a boundary layer totally uncorrelated with ORM (when the overpass is above the North African continent). For that simple reason the comparison CALIOP – ground lidar is meaningless for IOP2 and IOP3. During IOP1 two descendent overpasses are available: on 10JUL07 at 0227UTC at 917 km East of ORM over the North African continent, and on 11JUL07 at 0310UTC at 115 km West of ORM over the Atlantic Ocean. We have preferred here to draw symbolically the tracks of these two overpasses on the vertical cross-sections of dust concentration provided by DREAM in order to have simultaneously an estimation of the dust distribution horizontally and vertically. Fig. 10 shows the dust loading maps and the dust concentration vertical cross sections for the first two nights of the first IFC at 0000 UTC. The model predicts Saharan dust over ORM on both nights, even though always on the edge of the plume.

On the night of 9 – 10 July, CALIOP was compared to the UPC lidar in terms of attenuated backscatter profiles first at the nearest distance to the ground lidar (labelled 1 in Fig. 10a and Fig. 10c). Since 1) this was the beginning of the event and the dust had just started to be advected and transported and 2) Position 1 of CALIPSO is also on the edge of the plume (according to DREAM, Fig. 10a) we decided to perform the comparison for another position of CALIPSO more South. The first position of CALIOP South of Position 1 showing dust layers not contaminated by clouds was found at 23º N (labelled 2 in Fig. 10a and Fig. 10c), now at 1020 km Southeast of the ground lidar. The comparison of the attenuated backscatter of CALIOP at position 1 and 2 with the UPC lidar is shown in Fig. 11a and Fig. 11b at 532 and 1064 nm, respectively. As previously seen in Fig. 3a several layers are observed up to ~7.5 km asl on the UPC lidar profile. The profile of CALIOP at Position 1 also shows a multi-layer configuration and in particular two main layers which are much thinner and much lower than those observed by the UPC lidar. Since this is the very beginning of the event and Position 1 is on the edge of the plume according to the DREAM forecast, the dust advection at that time and place might be weaker in terms of dust concentration and altitude reached. However the morphology of the layers observed by CALIOP is similar to that observed by the UPC lidar. The profile of CALIOP at Position 2 shows a well developed layer from 3 to 8 – 9 km and clouds below 3 km. The order of magnitude of the dust layer is very similar to

that from the UPC lidar. CALIOP at both Position 1 and 2 succeeds in retrieving the dust layers which are the main responsible for the extinction above ORM. However, at the nearest position of CALIOP to the ground lidar, where the best correlation is expected, the vertical distribution shows important differences.

The equivalent plots for the night of 10 – 11 July are shown in Fig. 10b, Fig. 10d, Fig. 11c and Fig. 11d. The bottom part of Fig. 10d shows that longitudinally CALIOP is expected to observe the far West edge of the plume. However Fig. 11c and Fig. 11d which show the attenuated backscatter profile for both CALIOP and the UPC lidar clearly evidence that CALIOP is not observing the now well-mixed dust layer that the UPC lidar is detecting between 3 and 5.5 km. This emphasizes two important points: 1) on the edge of the plume the DREAM model may not be able to forecast accurately the dust horizontal and vertical distribution, and 2) CALIOP is not always reliable for retrieving long-range transport aerosols above ORM for the simple reason that it may be flying a few tens or hundreds of kilometres away from the position of the observatory.

6. CONCLUSION

An astronomical site has been characterized in terms of aerosol stratification and loading by means of an aerosol, backscatter lidar in the framework of the European project entitled "Extremely Large Telescope Design Study". To our knowledge it is the first time that results from such an experiment are presented. A total of 37 measurements of at least 30-min. duration were performed during two intensive field campaigns at the Roque de los Muchachos Observatory at 2395 m asl during 9 – 11 July 2007 and 26 May – 14 June 2008. Three main synoptic scenarios were identified bringing, supposedly, Saharan dust during the first campaign, marine/oceanic aerosols in the first half of the second campaign and European aerosols in the second half. Those three types of aerosols were classified according to their origin and permanence over continental landmasses and sea in previous works and already identified as the statistically more common plumes observed in ORM.

In all scenarios the lidar nocturnal cycles revealed a multi-layer stratification. The mean nocturnal PBL height is 546 m agl. This relatively high height is favourable to astronomical applications since for a fixed *AOT* **the higher the PBL height, the lower the aerosol concentration**. Between different intensive observation periods the PBL height does not change significantly but it does have a relatively large variability within the same IOP. The top layer was detected at 3268, 1983 and 4008 m agl during IOP1, IOP2 and IOP3, respectively. Low temperatures and strong winds measured during IOP2 at ground level explain partially the reduced vertical development of the layers above the PBL. During IOP3 (in the absence of Saharan dust transport) some top layers were detected as high as ~ 8400 m asl. The hypothesis is made that the combination of the exceptionally steep orography of La Palma island on its northern part and the prevailing winds from the northeast (Varela, Muñoz-Tuñon & Mahoney 1999) could act as a springboard to inject air masses to such high altitudes. Further investigation is needed to conclude on that hypothesis.

As far as aerosol loading is concerned, except in the presence of Saharan dust (IOP1) the *AOT* is very low: the average values are 0.051 and 0.03 at 532 nm and 0.008 and 0.003 at 1064 nm for IOP2 and IOP3, respectively. During the first part of the second IFC the *AOT* was approximately two to almost three times higher than in the second part whereas the highest aerosol layers were detected at lower altitude. **This indicates either a higher aerosol concentration in the first part of the campaign or a quite different (more absorbing) aerosol composition. Even though both explanations have a negative impact on astronomical observations because of the increase of the extinction at the observing wavelength, the AOT remains very low in both IOPs which characterizes extremely clean air.** Another possible

explanation might be the change in the relative humidity which at ground level was two to three times higher in the first part of the campaign compared to the rest of it. Additional reasons linked to the lidar inversion itself are also suspected: marine/oceanic aerosols observed in IOP2 have probably a lower LR than 30 sr, the value used in the inversions (that would reduce the *AOT* in IOP2), high error bars are associated to the lidar inversion products due to low signal-to-noise ratios. During IOP1 high *AOTs* were found due to the presence of Saharan dust: 0.233 and 0.157 at 532 and 1064 nm, respectively. The proportion of *AOT* contained in the PBL against that contained in the other layers above the PBL is very similar between both wavelengths: during IOP1, approximately 8 – 9 % of the column *AOT* is contained in the PBL, 50 – 54 % during IOP2 and 35 – 36 % during IOP3. **Even in the absence of Saharan dust the proportion of *AOT* contained in the layers above the PBL is either equal (IOP2) or larger (IOP3) than that contained in the PBL. This result indicates that the PBL is not the most important contributor of extinction due to aerosols.**

The lidar-derived *TOT* was also compared to the same quantity measured by the Carlsberg Meridian Telescope. During the first IFC the CMT-derived *TOT* remained relatively constant around 0.1172 while the lidar-derived *TOT* fluctuated between 0.123 and 0.186. No correlation was found between both quantities because of the mixing state of the aerosols and the hypothesis made by the method employed by the CMT that the aerosol extinction is not wavelength-dependent. During IOP1 a good correlation is obtained between both *TOTs* . **This demonstrates that for coarse aerosols, the most adverse to astronomical observations, the CMT instrument is able to estimate correctly the *TOT* independently of the wavelength.**

During IOP1 the ground lidar measurements were also compared to CALIOP profiles in order to evaluate the use of a spaceborne active instrument for aerosol content monitoring in an astronomical site. Two overpasses were considered. When CALIOP flew East of the ground lidar, CALIOP detected several layers with a morphology similar to that observed by the ground lidar but at lower altitudes and with weaker backscatter coefficients. When CALIOP flew West of the ground lidar, it did not detect the Saharan dust plume observed by the ground lidar. This first comparison of CALIOP profiles with a ground-based lidar over an astronomical site shows that it is essential that the orbit track be close to the site position to avoid pointing differences. The exceptionally steep orography of the island is also to be taken into account: in less than 9 km the island terrain rises from sea level up to 2395 m, the ORM altitude. In those conditions CALIOP, even only a few tens of kilometres apart from the ORM position, might observe aerosol layers totally uncorrelated with those observed above ORM. From its own nature, the aerosol content monitoring over an astronomical site requires very directive atmospheric soundings right above or in the very close vicinity of the site especially in the case of steep orography places. CALIOP is a suitable tool to monitor the presence of Saharan dust over ORM but it may lack of spatial precision (position of its overpass compared to the ORM position) and time resolution (revisiting time in a large range around the ORM position > 12 hours). In the absence of Saharan dust it is not able to monitor the aerosol stratification above ORM.

ACKNOWLEDGMENTS

This work is supported by the European Union under the projects “Technology development program towards a European Extremely Large Telescope” (ELT Design Study, EU Specific Support Action, contract nº 011863 (RIDS)), and EARLINET-ASOS (EU Coordination Action, contract nº 025991 (RICA)); by the MICINN (Spanish Ministry of Science and Innovation) and FEDER funds under the projects CIT-020400-2005-56 and CIT-020400-2007-67, the projects TEC2009-09106/TEC and TEC2006-07850/TCM, and the Complementary Action CGL2008-01330-E/CLI; and

by the European Space Agency under the project 21487/08/NL/HE. The authors gratefully acknowledge the Earth Sciences Division of the Barcelona Supercomputing Center for the DREAM maps, the NOAA Air Resources Laboratory (ARL) for the provision of the HYSPLIT transport and dispersion model and READY website (http://www.arl.noaa.gov/ready.html) used in this publication.

REFERENCES

Ansmann A., Wandinger U., Riebesell M., Weitcamp C., Michaelis W., 1992, Appl. Opt., 31, 7113

Ansmann A., Müller D., 2005, in Weitcamp C., ed, LIDAR—Range-Resolved Optical Remote Sensing of the Atmosphere, Springer, p. 112

Cuevas E., Baldasano J. M., Rodríguez S., Romero P. M., Alonso-Perez S., Basart S., Pérez C., 2009, Report AEMET / BSC-CNS

Doherty S. J., Anderson T. L., Charlson R. J., 1999, Appl. Opt., 38, 1823

Draxler R.R., Rolph G.D., 2003, http://www.arl.noaa.gov/ready/hysplit4.html, NOAA Air Resources Laboratory, Silver Spring, MD

Fernald F. G., 1984, Appl. Opt., 23, 652

Garcia-Gil A., Muñoz-Tuñón C, Varela A.M, 2009, 2009, PASP to be submitted

Guerrero M.A., García-López R.J., Corradi R.L.M., Jiménez A., Fuensalida J.J., Rodríguez-Espinosa J.M., Alonso A., Centurión M., Prada F., 1998, New Astronomy Reviews, 42, 529

Jones D. H. P., 1984, RGO/La Palma Technical Note 10

Kalnay E., Kanamitsu M., Kistler R., Collins W., Deaven D., Gandin L., Iredell M., Saha S., White G., Woollen J., Zhu Y., Chelliah M., Ebisuzaki W. Higgins W., Janowiak J., Mo K. C., Ropelewski C., Wang J., Leetmaa A., Reynolds R., Jenne R., Joseph D., 1996, Bull. Amer. Meteor. Soc., 77, 437

King D. L., 1985, RGO/La Palma Technical Note 31

Klett J. D., 1981, Appl. Opt., 20, 211

Landulfo E., Papayannis A., Artaxo P., Castanho A. D. A., de Freitas A. Z., Sousa R. F., Vieira Junior N. D., Jorge M. P. M. P., Sánchez-Ccoyllo O. R., Moreira D. S., 2007, Atmos. Chem. Phys. Discuss., 3, 2835

Mona L., Amodeo A., Pandolfi M., Pappalardo G., J. Geophys Res., 111, D16203

Nickovic S., Papadopoulos A., Kakaliagou O., Kallos G., 2001, J. Geophys. Res., 106, 18113

Papayannis A., Amiridis V., Mona L., Tsaknakis G., Balis D., Bösenberg J., Chaikovski A., De Tomasi F., Grigorov I., Mattis I., Mitev V., Müller D., Nickovic S., Pérez C., Pietruczuk A., Pisani G., Ravetta F., Rizi V., Sicard M., Trickl T., Wiegner M., Gerding M., Mamoury R., Di Amico G., Pappalardo G., 2008, J. Geophys. Res., 113, D10204

Rocadenbosch F., Sicard M., Comerón A., Baldasano J.M., Rodríguez A., Agishev R., Muñoz C., López M.A., García-Vizcaino D., 2002, Proc. 21st International Laser Radar Conference, vol. 1, p. 69

Rolph G.D., 2003 http://www.arl.noaa.gov/ready/hysplit4.html, NOAA Air Resources Laboratory, Silver Spring, MD

Sasano Y., Nakane H., 1984, Appl. Opt., 23, 11

Shettle E. P., Fenn R. W., 1979, Envisonmental Research paper No. 675, AFGL-TR-79-0214, NTIS, ADA 085951

Sicard M., 2000, PhD thesis, Univ. Paris 7 Denis Diderot

Sicard M., Pérez C., Rocadenbosch F., Baldasano J.M. , García-Vizcaino D., 2006, Boundary-Layer Metorol., 119, 135

Sicard M., Tomás S., Comerón A., Rocadenbosch F., Rodríguez A. Muñoz C. Batet O., 2008, Proc. IEEE International Geoscience and Remote Sensing Symposium, vol. 3, p. 915

Sicard M., Tomás S., Md Reba M. N., Comerón A., Batet O., Muñoz-Porcar C., Rodriguez A., Rocadenbosch F., Muñoz-Tuñón C., Fuensalida J. J., 2009, Proc. SPIE Europe Remote Sensing, in press

Stull, R. B., 1988, Kluwer Academic Publishers, Dordrecht, The Netherlands, 670 pp.

Toledano C., Cachorro V. E., Berjon A., de Frutos A. M., Sorribas M., de la Morena B. A., Goloub P., Q. J. R. Meteorol. Soc., 133, 795

Varela A. M., Muñoz-Tuñon C., Mahoney T., 1999, Ap&SS, 263, 373

Varela A. M., Bertolin C., Muñoz-Tuñón C., Ortolani S., Fuensalida J.J., 2008, MNRAS, 391, 507

Winker D., Pelon J., McCormick M. P., 2006, Proc. 23rd International Laser Radar Conference, p. 991

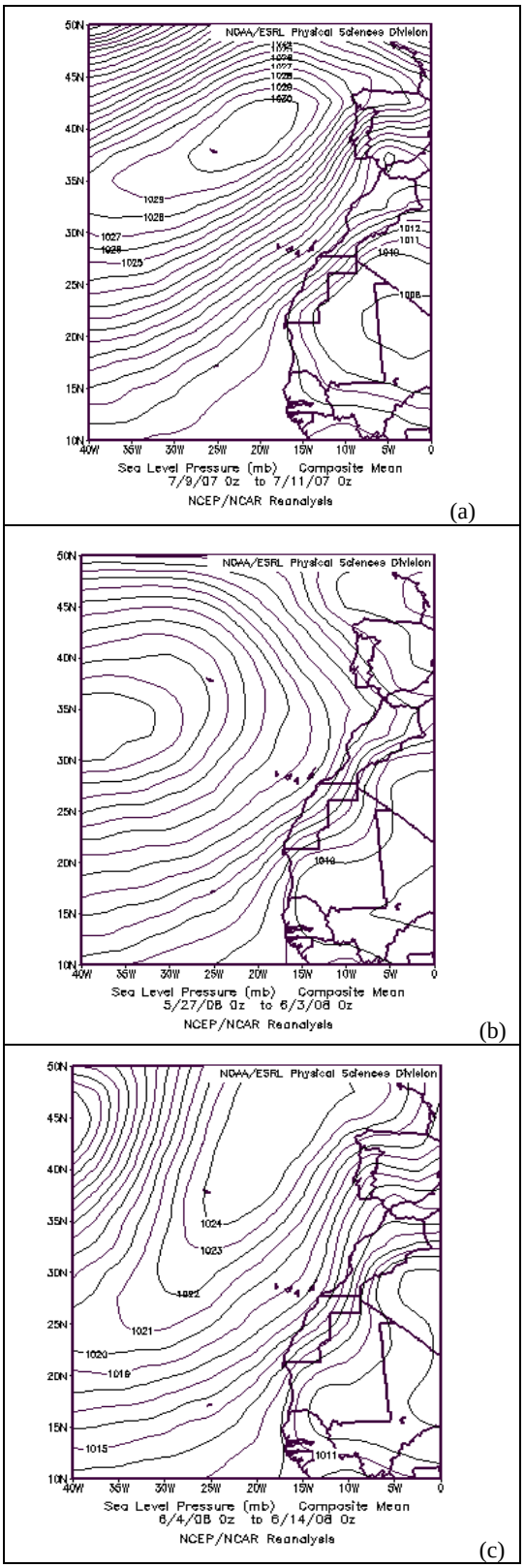

Fig. 1. Sea level pressure at 0000UTC averaged over the period (a) 09JUL07-11JUL07, (b) 27MAY08 – 02JUN08, and (c) 03JUN08 – 14JUN08.

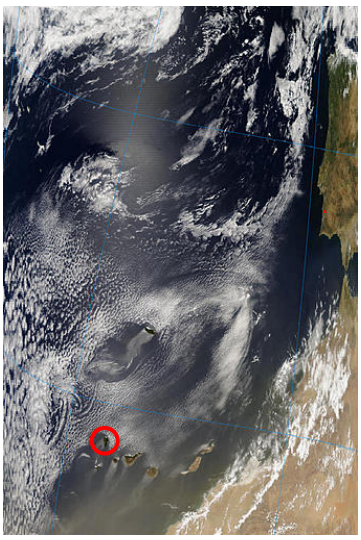

Fig. 2. 4-km resolution image of MODIS aboard AQUA satellite taken on 11JUL07 at 1415UTC. The island of La Palma is surrounded by a red circle.

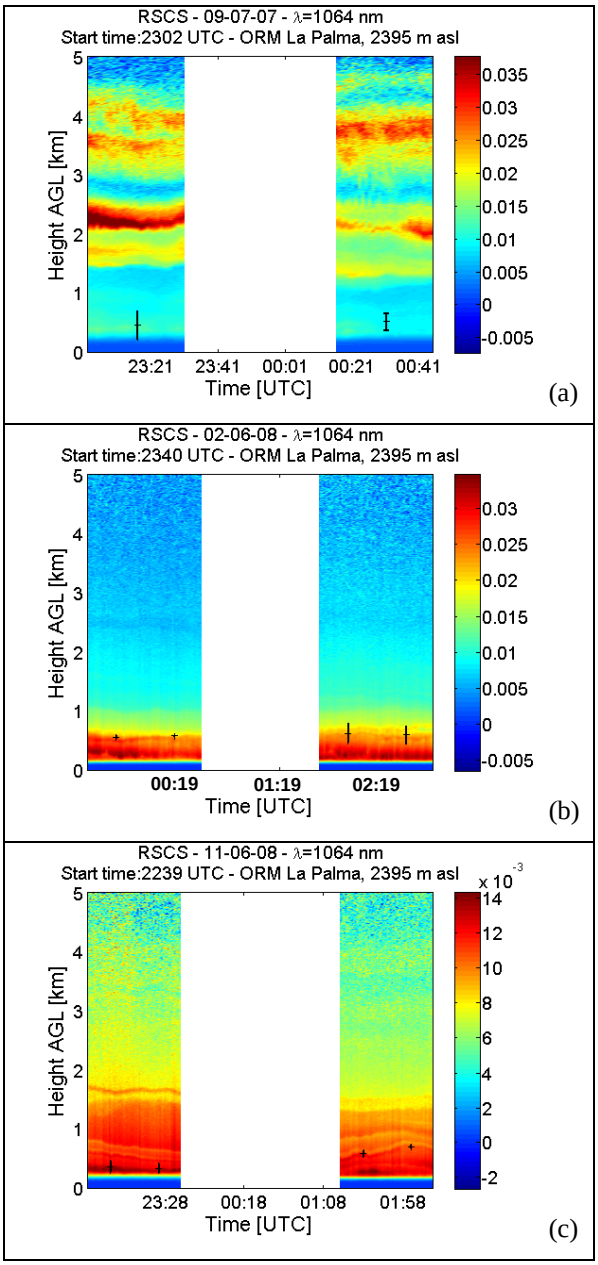

Fig. 3. Temporal evolution of the RSCS on (a) 09JUL07, (b) 02JUN08 and (c) 11JUN08. The PBL height is indicated by '+' signs. The error bar associated to the PBL height was computed as the standard deviation of the 30 profiles used to calculate the mean PBL height.

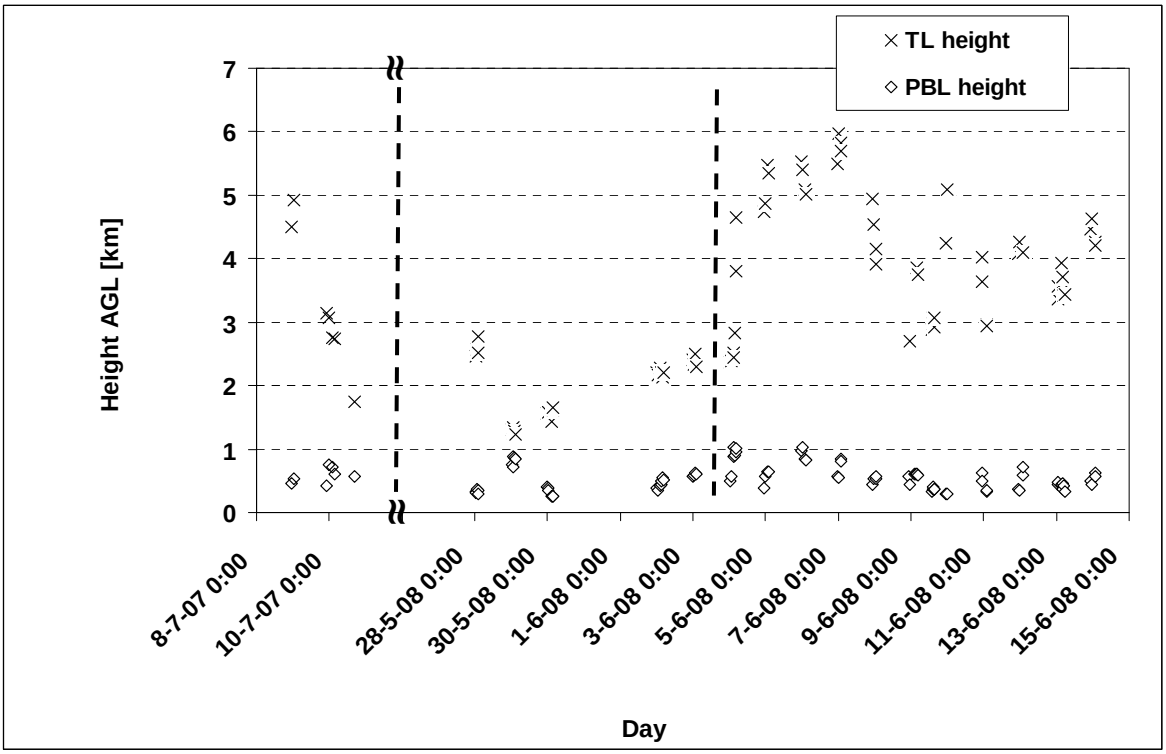

Fig. 4. Temporal evolution of the PBL height and the TL height.

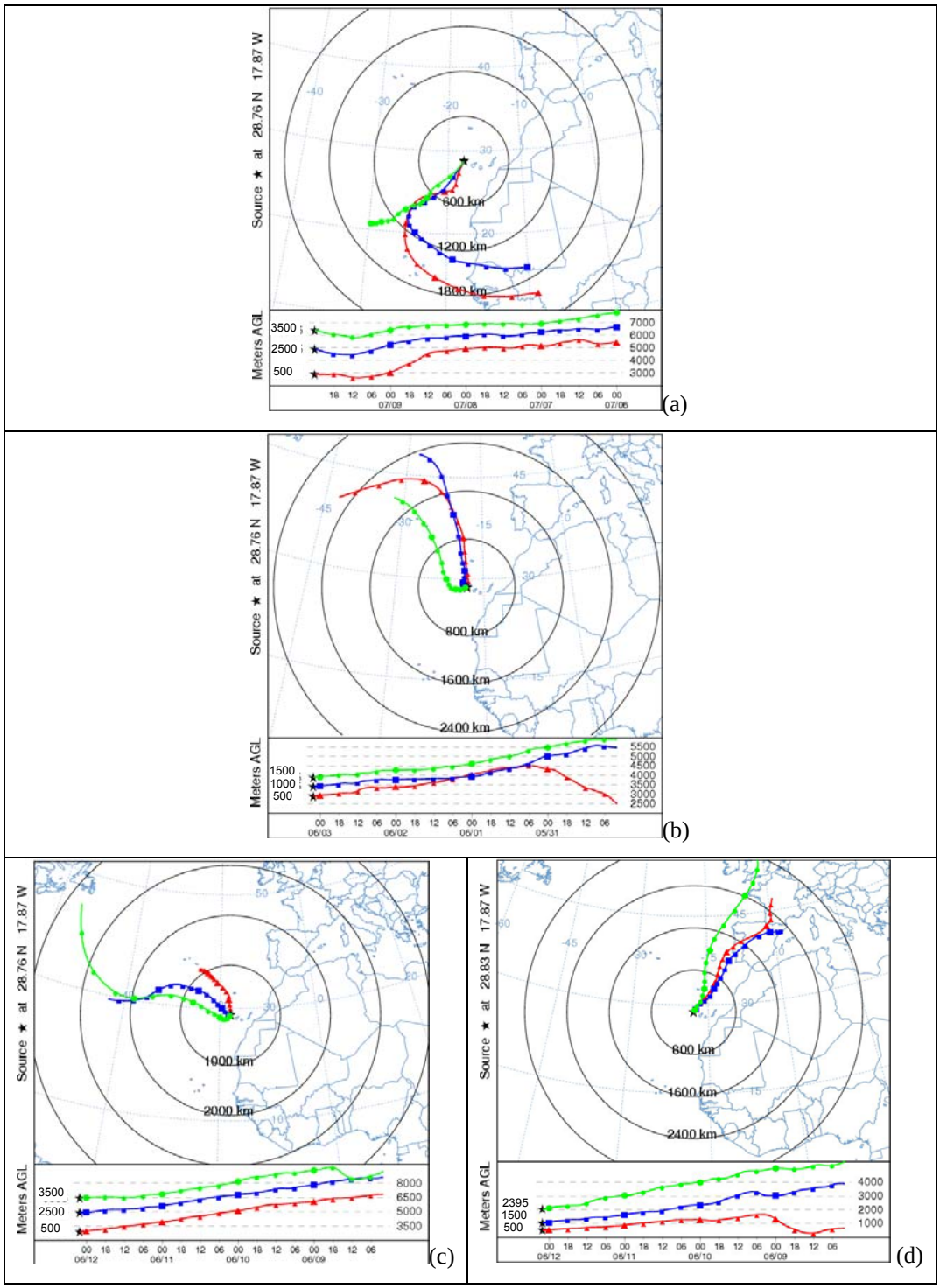

Fig. 5. Hysplit backtrajectories arriving at ORM (2395 m agl) on (a) 10JUL07 at 0000UTC, (b) 03JUN08 at 0200UTC, and (c) 12JUN08 at 0200UTC, and (d) arriving at the nearest coast (0 m agl) from ORM on 12JUN08 at 0200UTC.

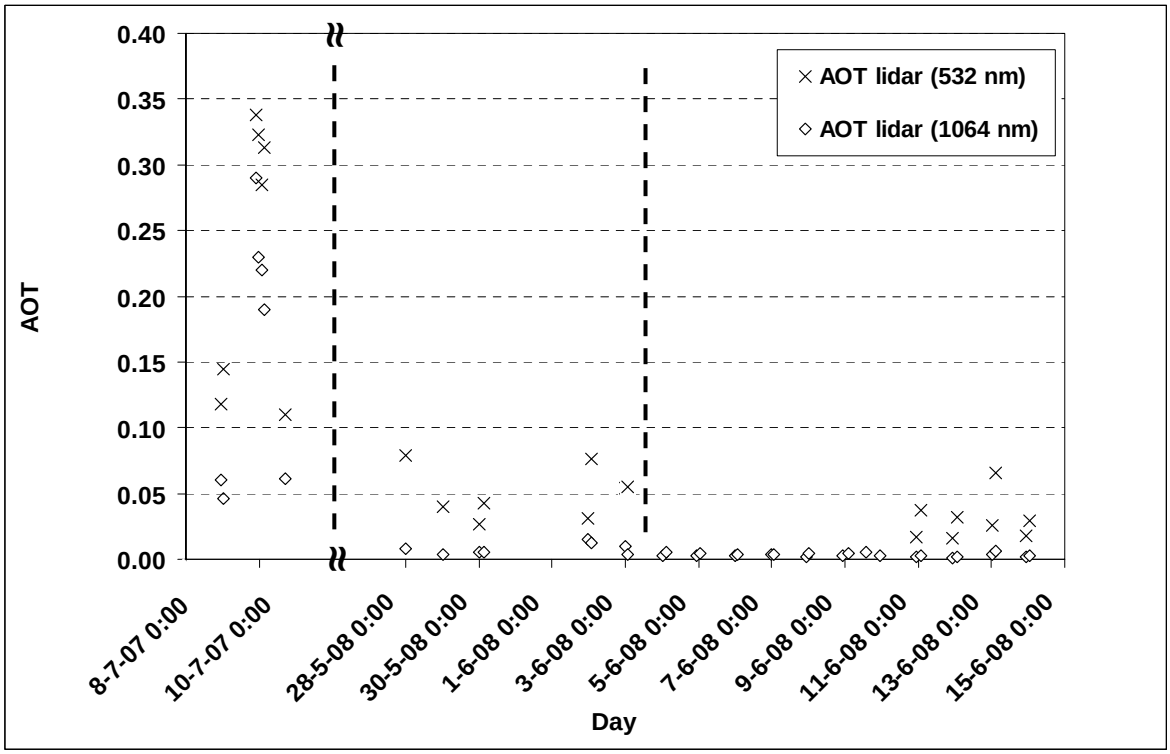

Fig. 6. Temporal evolution of the lidar-derived *AOT* .

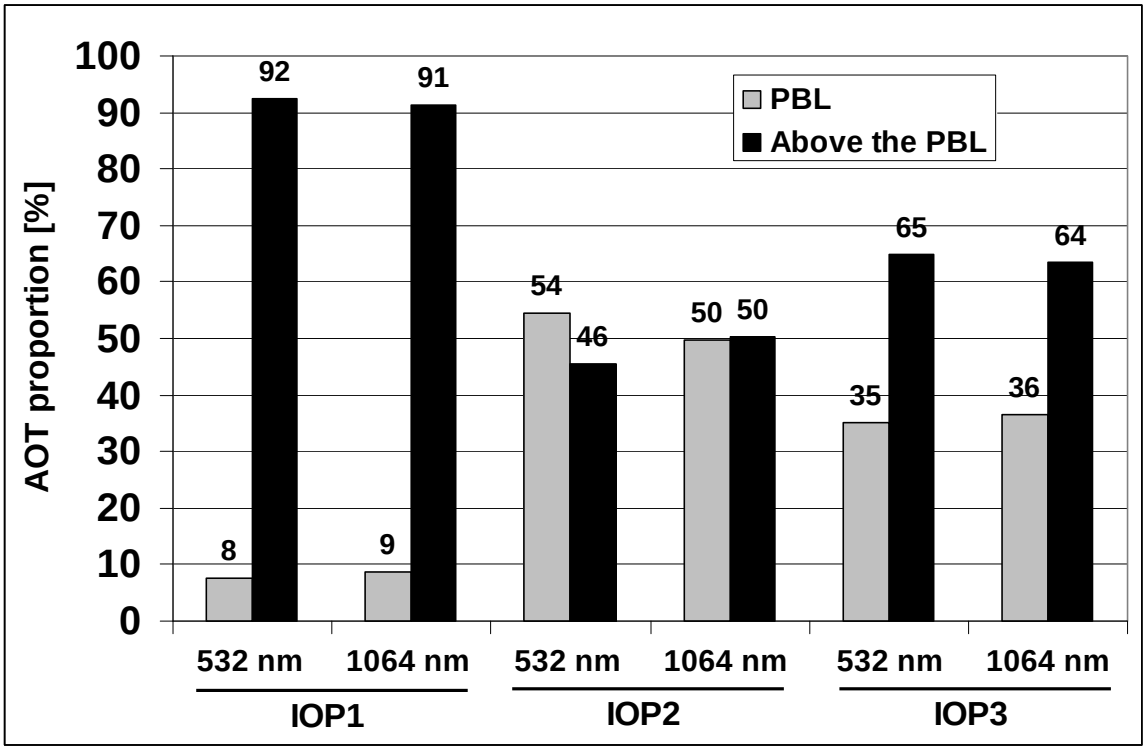

Fig. 7. Percentage of the *AOT* contained in the PBL and in the layers above the PBL in the 3 synoptic situations found and at both wavelengths of 532 and 1064 nm.

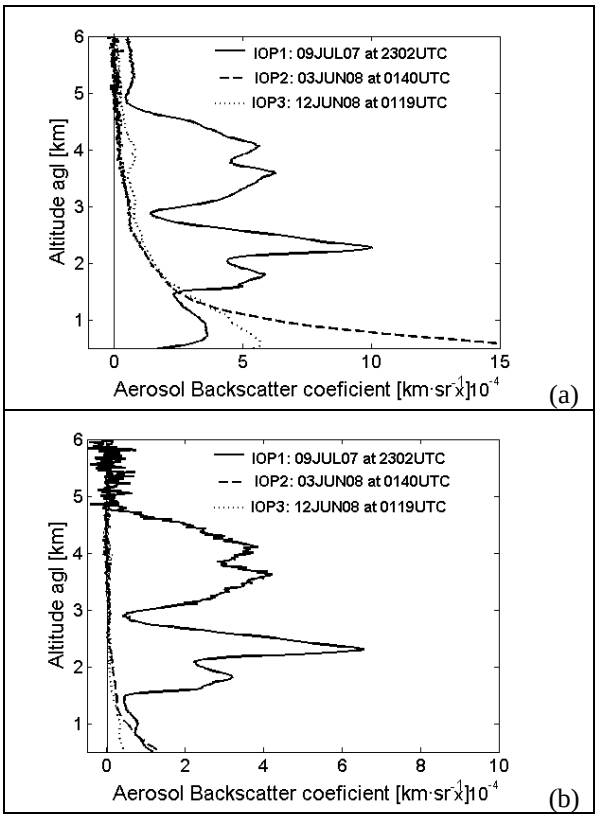

Fig. 8. Aerosol backscatter coefficient at (a) 532 nm and (b) 1064 nm. The *AOT* at 532 nm for 09JUL07, 03JUN08 and 12JUN08 is 0.118, 0.055 and 0.032, respectively. At 1064 nm it is 0.06, 0.0039 and 0.0022, respectively.

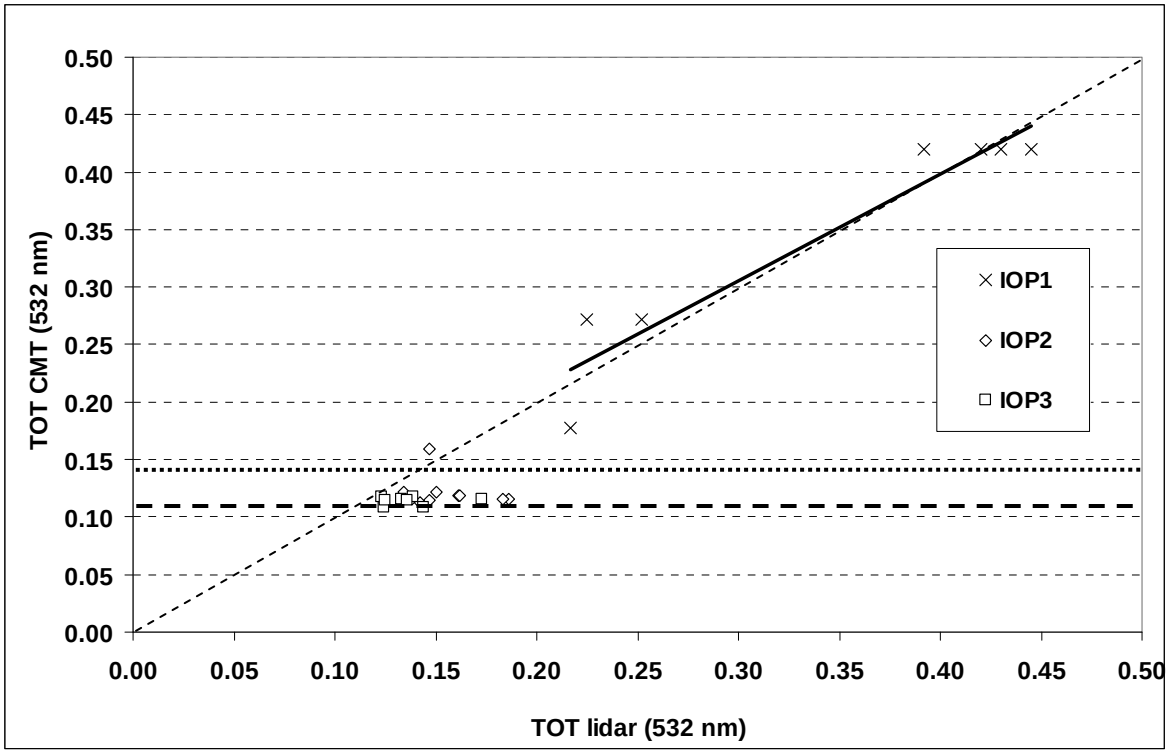

Fig. 9. CMT-derived vs. lidar-derived *TOT* at 532 nm. The dashed and dotted horizontal lines indicate the CMT-derived *TOT* (532 nm) limits for no atmospheric extinction at all (0.1105, conversion in *TOT* of 0.12 mag·aimass^{-1}) and Saharan dust presence (0.1409, conversion in *TOT* of 0.153 mag·aimass^{-1}), respectively. The solid black line corresponds to the best fit between lidar- and CMT-derived *TOT* for IOP1.

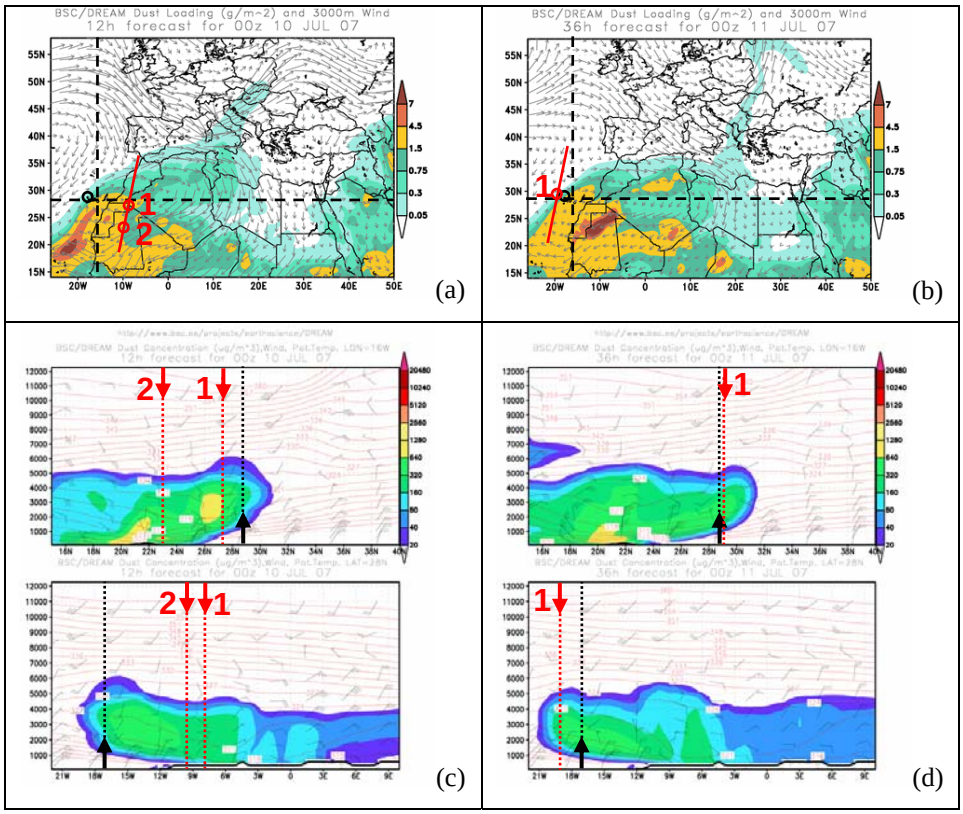

Fig. 10. Dust loading map and synoptic wind at 3000 m asl forecast by DREAM at 0000UTC on (a) 10JUL07 and (b) 11JUL07. The island of La Palma is surrounded by a black circle. The red line indicates the CALIPSO overpass (a) on 10JUL07 at 0227UTC and (b) on 11JUL07 at 0310UTC. The red circles labelled 1 indicate the closest position of CALIPSO compared to the lidar position. On 10JUL08 a second position labelled 2 at latitude 23º N is also indicated by a red circle. The vertical cross sections of dust concentration up to 12 km at longitude 16º W and latitude 28º N are also plotted for (c) 10JUL07 and (d) 11JUL07. The black and red vertical lines indicate the UPC lidar and the CALIOP positions, respectively.

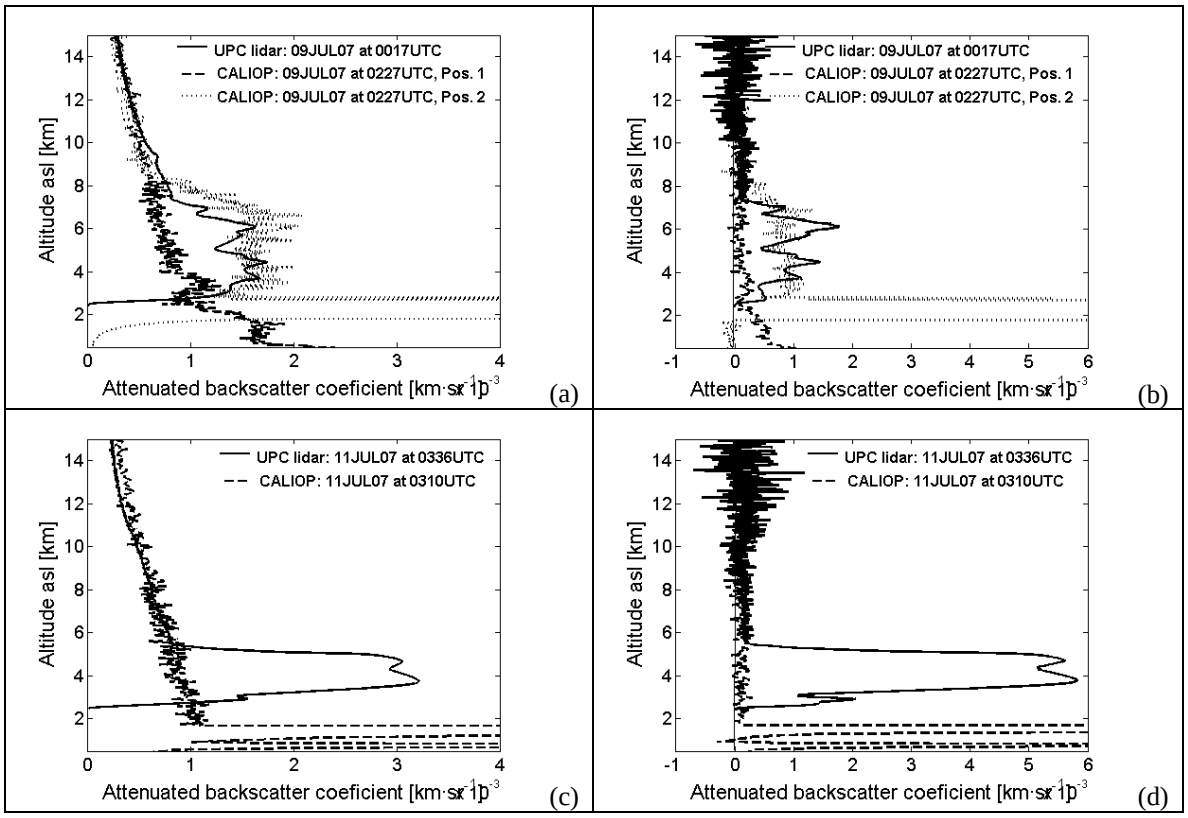

Fig. 11. Total attenuated backscatter coefficient on 09JUL07 at (a) 532 and (b) 1064 nm, and on 11JUL07 at (c) 532 and (b) 1064 nm. The lidar-derived *AOT* on 09JUL07 is 0.145 and 0.046 at 532 and 1064 nm, respectively. On 11JUL07 it is, respectively, 0.313 and 0.19.

		DAY									DAY + 1						CALIPSO
		13:00	14:00	15:00	16:00	17:00	...	21:00	22:00	23:00	0:00	1:00	2:00	3:00	4:00	5:00	overpass
IOP1	09/07/2007									23:02	0:17						2:27
	10/07/2007									23:03 23:32		1:41		3:36			3:10
	11/07/2007				16:51												
IOP2	27/05/2008										0:13						3:05
	28/05/2008											0:31					
	29/05/2008									23:55				3:06			
	30/05/2008																
	31/05/2008																
	01/06/2008									23:49			2:08				3:24
	02/06/2008									23:40		1:40					
IOP3	03/06/2008										0:24			2:34			3:11
	04/06/2008								22:47			0:50					
	05/06/2008									23:44		1:52					
	06/06/2008									23:23		1:24					
	07/06/2008		~~13:57~~						22:41			0:28					14:41
	08/06/2008								22:09				2:15				3:30
	09/06/2008		13:30							23:11							14:29
	10/06/2008								22:29		1:28						
	11/06/2008								22:39			1:19					
	12/06/2008											0:31		3:02			3:05
	13/06/2008								22:29			1:11					

Table 1. Schedule of the measurements made at zenith during the IFCs. The time is in UTC and indicates the starting time of the measurement. All regular measurements are 30- or 60-min. long; CALIOP correlative measurements are 150-min. long and are indicated by dotted cells. At 1357UTC on 09JUN08 the striped cell indicates profiles not usable because of acquisition problems. CALIPSO overpasses are indicated in the far right column. The CALIOP daytime and nighttime measurements correspond to DAY and DAY+1, respectively.

	Layer height				AOT at 532 nm			AOT at 1064 nm		
	PBL	Std dev. PBL	TL	Std dev. TL	PBL	Ab. PBL	Column	PBL	Ab. PBL	Column
	(m)	(m)	(m)	(m)	()	()	()	()	()	()
IOP1	0.581	0.186	3.268	0.480	0.018	0.215	0.233	0.017	0.140	0.157
IOP2	0.487	0.192	1.983	0.490	0.028	0.022	0.051	0.004	0.004	0.008
IOP3	0.571	0.204	4.008	0.970	0.011	0.019	0.030	0.001	0.002	0.003
Overall	0.546	0.198	3.343	1.254	0.019	0.080	0.099	0.005	0.028	0.033

Table 2. Mean height of both the PBL and the TL detected by the lidar, as well as the *AOT* at 532 and 1064 nm in the PBL, above the PBL and in the whole column.